J. Phys. B: At. Mol. Opt. Phys. **29** (1996) 2355–2366. Printed in the UK

Electron-impact-induced emission cross sections of neon in the extreme ultraviolet

I Kanik, J M Ajello and G K James
Jet Propulsion Laboratory, California Institute of Technology, Pasadena, CA 91109, USA

Received 25 August 1995, in final form 25 January 1996

Abstract. We have measured the extreme ultraviolet (EUV) spectrum of neon produced by electron impact excitation. The measurements were obtained under optically thin conditions, and at a spectral resolution of 0.5 nm full width at half maximum (FWHM). The most prominent features of the EUV spectrum between 45–80 nm are the resonance lines of Ne I at 73.6 and 74.4 nm and a multiplet of Ne II at 46.14 nm (the average value for the line centre of the two closely spaced ion lines at 46.07 and 46.22 nm). Absolute emission cross sections of these lines at 300 eV were measured and compared to other previous measurements. The measured emission cross section values at 300 eV for the Ne I lines at 73.6 and 74.4 nm are found to be 5.32×10^{-18} cm^2 and 1.21×10^{-18} cm^2 respectively, and for the Ne II multiplet at 46.14 nm is found to be 1.53×10^{-18} cm^2 (sum of the 46.07 and 46.22 nm line cross sections) with an uncertainty of 41%. In addition, excitation functions were measured for the Ne I resonance lines (0–400 eV) and Ne II ion line (0–1 keV). The excitation functions for the Ne I resonance lines were corrected for polarization because these are strongly polarized.

1. Introduction

Electron-impact-induced emission studies of Ne are of considerable importance in understanding the basic physics of collisional excitation processes and in technological applications. From the basic physics point of view, Ne is part of the rare-gas series, and like other rare-gas atoms is of special interest because Ne has a large number of excited levels. Also, the simple LS and jj coupling schemes are not strictly applicable for neon (Chan *et al* 1992). The LS coupling breaks down and changes into jl coupling and then to jj coupling in the spectroscopic description of the states of this atomic system (Machado *et al* 1984). From the applied physics point of view, Ne plays an important role in many discharge systems such as Ne-discharge light sources, He–Ne lasers, and Ne–Xe–NF_2 lasers (Nighan 1981, Huentis *et al* 1978). Knowledge of the excitation cross sections is therefore essential for modelling these discharge systems (Phillips *et al* 1985). Neon also plays an important role in astrophysics since it is the most abundant of the rare gases in the solar system, and in the cosmos after helium. Its spectroscopic detection in the atmospheres of the outer planets, which are expected to reflect solar abundance, has eluded astronomers (Atreya 1986). However, the recent astrophysical discovery of hot neon nova has occurred because of the rich spectra from highly ionized lines of neon (Barger *et al* 1993). At low temperatures, the importance of the EUV spectrum of neutral neon and its singly and doubly charged ions from cool stellar atmospheres has been considered by Landini *et al* (1985). Their models of EUV surface fluxes of stellar objects are limited by accurate knowledge of plasma emissivities. The main problem in the calculation of the plasma emissivity is the

0953-4075/96/112355+12$19.50

unavailability of accurate excitation cross sections for electron impact. The need for the measurement of electron impact excitation cross sections for Ne in modelling astrophysical plasmas is pointed out by Shull (1993).

In this paper, the electron-impact-induced emission spectrum of Ne corresponding to the resonance transitions in the EUV spectral region from 45–80 nm at 300 eV impact energy is reported. (In a companion paper we have reported emission cross sections of Ne II and Ne III excited by electron impact, measured in the far ultraviolet (FUV) spectral region from 120–270 nm (James *et al* 1995).) Absolute emission cross sections corresponding to the Ne spectral features (Ne I, Ne II and Ne III) in the 45–80 nm region were measured. Previous work concerning electron-impact excitation of Ne in the 45–80 nm wavelength region is reviewed and a comparison of our results for absolute emission cross sections of Ne emission features (resonance and ion lines) with those of the previous work is given. Ne, like other heavier noble gases, provides important resonance lines of the type $n\mathrm{p}^5(n+1)\mathrm{s} \rightarrow n\mathrm{p}^6$, and ion lines of the type $ns n\mathrm{p}^6 \rightarrow ns^2 n\mathrm{p}^5$. The 73.59 nm and 74.37 nm resonances lines of Ne I and 46.07 nm and 46.24 nm resonance lines of Ne II represent the transitions between the lowest-lying electronic excited states and the ground state of the atom and ion, respectively. Optical excitation functions were also measured for the Ne I (73.59 nm) $2\mathrm{p}^5[^2\mathrm{P}_{1/2}]3\mathrm{s}(^1\mathrm{P}_1) \rightarrow 2\mathrm{p}^6(^1\mathrm{S}_0)$ and Ne I (74.37 nm) $2\mathrm{p}^5[^2\mathrm{P}_{3/2}]3\mathrm{s}(^3\mathrm{P}_1) \rightarrow 2\mathrm{p}^6(^1\mathrm{S}_0)$ resonance transitions which have predominantly singlet and triplet characters, respectively. In addition, the optical excitation function for the unresolved multiplet of Ne II ($46.07 + 46.22$ nm) $2\mathrm{s}(^2\mathrm{S}_{1/2})2\mathrm{p}^6 \rightarrow 2\mathrm{s}(^2\mathrm{P}_{3/2,1/2})2\mathrm{p}^5$ transition, which results from the removal of a 2s electron and subsequent decay to the ion ground state, was measured.

The ground level of Ne is $1\mathrm{s}^2 2\mathrm{s}^2 2\mathrm{p}^6\ ^1\mathrm{S}_0$. The lowest excited configuration is $1\mathrm{s}^2 2\mathrm{s}^2 2\mathrm{p}^5 3\mathrm{s}$, which yields four energy levels. These levels are $1\mathrm{s}_2, 1\mathrm{s}_3, 1\mathrm{s}_4$ and $1\mathrm{s}_5$ in Paschen notation (Register *et al* 1984). The $1\mathrm{s}_3$ and $1\mathrm{s}_5$ levels are metastable with very long radiative lifetimes. Electron-impact-induced emission resulting from radiative decay from these levels to the ground state, therefore, cannot be measured by conventional optical methods. The $1\mathrm{s}_2$ level is primarily $^1\mathrm{P}_1$ in character, with less than 10% admixture of $^3\mathrm{P}_1$, and *vice versa* for the $1\mathrm{s}_4$ level (Phillips *et al* 1985). The transitions from these levels ($1\mathrm{s}_2$ and $1\mathrm{s}_4$) to the ground state represent the strongest resonance transitions in the vacuum ultraviolet (VUV), and occur at 73.6 and 74.4 nm, respectively. Direct cascade to these resonance levels comes from the $2\mathrm{p}^5 3\mathrm{p}$ group ($2\mathrm{p}_1$–$2\mathrm{p}_{10}$ in Paschen notation). Figure 1 shows a simplified level diagram for the Ne I 73.6 and 74.4 nm resonance transitions and for the Ne II 46.1 and 46.2 nm transitions.

The two most recent surveys of electron-impact-induced emission cross section and optical excitation function measurements for the resonance transitions for Ne have been published by van der Burgt *et al* (1989) and by Heddle and Gallagher (1989) for the EUV spectral region. Early measurements included those of Hertz (1969) who reported the Ne I (73.6, 74.4 nm) optical excitation functions, and those of de Jongh (1971) who measured the polarization-free optical excitation function for the Ne I (73.6 nm) resonance transition. Later, Luyken *et al* (1972) and van Raan *et al* (1973) reported cross sections for the Ne II ($46.1 + 46.2$ nm) ion lines. Tan *et al* (1974) measured the Ne I (73.6 nm) photoemission cross section, normalized to an average of experimental values for the oscillator strength for this transition. Zapesochnyi *et al* (1974) reported optical excitation functions for the Ne II ($46.1+46.2$ nm) transitions. They normalized their cross sections based upon the first Born approximation. Papp *et al* (1977) measured optical excitation functions for the Ne III (37.9, 49.0 nm) transitions. Dijkkamp and de Heer (1981) reanalysed the Ne II ($46.1 + 46.2$ nm) cross section from Luyken *et al* (1972). They put the cross section on an absolute scale using the Bethe approximation (Bethe 1930), which led to a cross section 3.7 times smaller

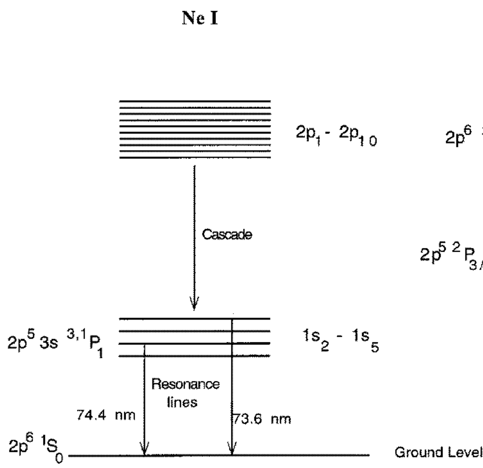

Figure 1. A simplified level diagram for the prominent transitions of Ne I and Ne II is shown. On the left-hand side, the electron configuration with terms and levels are indicated for Ne I and Ne II. On the right-hand side, the terms are given in Paschen notation for Ne I.

than that obtained based on a normalization utilizing the van Raan result (1973). Eckhardt and Schartner (1983) reported photoemission cross sections for the Ne II (46.1 + 46.2 nm) and Ne III (49.0 nm). Their cross sections are based on the Bethe approximation (Bethe 1930), with experimental and theoretical values for the optical oscillator strengths from Kim and Inokuti (1968) and de Jongh and van Eck (1971). Phillips *et al* (1985) measured the Ne I (73.6 and 74.4 nm) cross sections utilizing a laser-induced fluorescence technique. They normalized to the Born approximation and determined the cascade contribution by direct measurement. Register *et al* (1984) reported differential cross sections (DCSs) for excitation of 16 features in the electron energy-loss spectrum of Ne corresponding to individual level excitations (some unresolved). By integrating their measured DCSs, they obtained the integral cross sections for direct excitation without the cascade contribution which hampers the analysis of optical Ne data. Investigators (Tan *et al* 1974, Phillips *et al* 1985) reported the existence of large cascade components which contributed to the emission cross sections of the two resonance lines at 73.6 and 74.4 nm. Tan *et al* (1974) assumed that the cascade population of the Ne $^1P_1$ level at 73.59 nm varies with electron-impact energy as E^{-1}, whereas Phillips *et al* (1985) determined the cascade population by direct measurement. Phillips *et al* (1985) measured the emission cross sections of the two resonance lines at 300 eV electron-impact energy, resulting in a cascade contribution of 29%. For 40 eV, they estimated a total cascade contribution of 36% for the 73.6 and 74.4 nm resonance lines.

2. Experimental procedure

The experimental apparatus, calibration procedure and cross section measurement technique have been described in our earlier publications (Ajello *et al* 1988, 1989, Kanik *et al* 1995). The medium-resolution 1.0 m spectrometer system was used in the present measurements. It consists of an electron-impact collision chamber in tandem with a UV spectrometer. The EUV emission spectrum of Ne was measured by crossing a magnetically collimated beam of electrons with a beam of Ne gas formed by a capillary array. Emitted photons, corresponding to radiative decay of collisionally excited states of Ne, were detected at 90° by the UV spectrometer equipped with a channeltron detector. The resulting emission spectrum, measured at 300 eV incident electron beam energy, was calibrated for wavelength from 45 to 80 nm according to the procedures described by Ajello *et al* (1989). The laboratory measurements, together with the spectroscopic models, permitted the EUV spectrum from H_2 Rydberg series to serve as a relative calibration standard in the 80–230 nm range. For shorter wavelengths (40–80 nm) the $n^1P^o n = 2, 3, 4$ Rydberg series of He and Ar I and Ar II multiplets were used as the calibration source. In order to determine the absolute value of the emission cross section corresponding to each measured feature, one additional procedure (normalization) must be applied. The determination of the absolute emission cross sections for Ne was achieved by admitting a research grade gas mixture (purchased from a commercial source) containing 50% Ne and 50% N_2 into the scattering chamber and measuring the fluorescence signal from the gas mixture ($Ne + N_2$). Static gas ($Ne + N_2$) mode was utilized to maintain the same number density for Ne and N_2 in the target region during the measurements. Accuracy of the gas mixture is 99.995% as stated by the manufacturer. The relative cross sections for each feature were obtained by integrating the signal intensity over the wavelength interval for the feature of interest, and by then comparing the integrated signal intensity for each Ne spectral feature to that of the N_2 c_4 $^1\Sigma_u^+(0, 0)$ 95.8 nm fluorescence signal at 300 eV electron impact energy. The absolute cross section of the 95.8 nm spectral feature of N_2 at 300 eV impact energy (Ajello *et al* 1989) was then used to normalize the relative intensities of the Ne spectral features. A background gas pressure about 1.0×10^{-6} Torr was used to avoid the effect of self-absorption on the Ne resonance lines as discussed below. It should be pointed out here that the Ne background gas pressure was measured by an ion gauge and the ion gauge readings were corrected for the relative sensitivity of ion gauge response data for Ne (Bartmess and Georgiadis 1983).

The background gas pressure for the present determination of Ne emission cross sections was carefully chosen to ensure optically thin conditions and to avoid self-absorption effects, particularly for the Ne I resonance lines at 73.59 and 74.37 nm. The following approach has been employed to determine the maximum background gas pressure that can be used while maintaining optically thin conditions. The relative intensities of the Ne I resonance line (73.59 nm) and the Ne II ion line (46.1 + 46.2 nm) have been measured as a function of pressure over the range 3×10^{-7} to 2×10^{-4} Torr. The Ne II line is not expected to exhibit any optical depth effects in this pressure range and therefore acts as a normalization feature. The experimentally determined intensity ratio of these features is shown in figure 2, and is approximately constant up to a background gas pressure of 5×10^{-6} Torr where it begins to decrease. This indicates the onset of self-absorption at 73.59 nm. The measurement can be verified by calculating the pressure for optical depth unity at line centre for the strongest resonance line (Ne I at 73.6 nm). The optical depth, τ_0, at line centre is given by

$$\tau_0 = \sigma_0 n l \tag{1}$$

where σ_0 is the absorption cross section at line centre, n is the number density of the absorbing gas, and l is the path length (16.83 cm) from the collision volume to the spectrometer entrance slit. The absorption cross section value of 3.529×10^{-13} cm^2 at line centre, determined by using the oscillator strength (0.159) for the Ne I 73.6 nm resonance transition at 300 K (Chan *et al* 1992), is used to obtain the pressure corresponding to optical depth unity at line centre. The value of the pressure is found to be 5.2×10^{-6} Torr, which supports our experimental determination for the onset of self-absorption of the Ne I 73.6 nm resonance line (figure 2).

The measurements reported here were obtained at an angle of 90° between electron beam axis and optic axis. The Ne II resonance lines ($^2S_{1/2} \rightarrow {}^2P_{1/2,3/2}$) are unpolarized

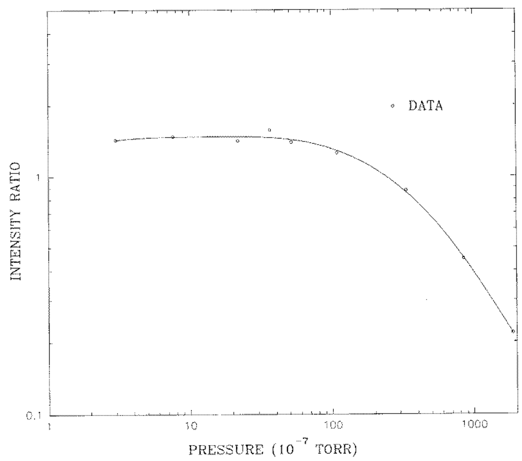

Figure 2. The intensity ratio of the Ne I resonance line at 73.6 nm and the Ne II ion multiplet at 46.14 nm as a function of Ne gas pressure. The ratio is approximately constant up to about 2×10^{-6} Torr and starts decreasing, indicating the onset of self-absorption of Ne I resonance line at 73.6 nm. The Ne II feature at (46.1–46.2 nm), which exhibits no optical depth, acts as a normalization feature.

and unaffected by self-absorption. However, the Ne I resonance lines ($^1P_1 \rightarrow {}^1S_0$ and $^3P_1 \rightarrow {}^1S_0$) are strongly polarized, as measured in the E_T–480 eV energy range (where E_T indicates the threshold energy) by Hammond *et al* (1989). The polarization was measured to be zero at 300 eV. For this reason, we studied the electron-impact-induced fluorescence spectrum of Ne at 300 eV. We measured the polarization-free optical excitation function of the Ne II (46.1 + 46.2 nm) lines in the electron-impact energy range 0–1 keV. The excitation functions for the strongly polarized Ne I (73.69 nm and 74.37 nm) lines were also measured in the 0–400 eV impact energy range, and these were corrected for polarization based on the Hammond *et al* (1989) polarization data.

3. Results and discussion

3.1. The EUV spectrum

Figure 3 shows the Ne laboratory emission spectrum in the EUV spectral region at 300 eV electron-impact energy in the wavelength range of 45–80 nm. The spectrum was obtained at a gas temperature of 300 K, under optically thin conditions, at a spectral resolution of 0.5 nm FWHM, and calibrated for wavelength. The background pressure was 5×10^{-7} Torr. The emission spectrum of Ne consists of eight spectral features. Table 1 lists the candidate identifications and the measured absolute emission cross sections corresponding to Ne I, II and III transitions at 300 eV electron-impact energy. The identifications were taken from Kelly (1987).

The Ne I (73.6 nm) resonance transition represents the strongest feature in the Ne EUV spectrum at 300 eV electron-impact energy. A comparison of the Ne I (73.6 nm) absolute emission cross section values indicates good agreement between the present determination and those of Tan *et al* (1974) and Phillips *et al* (1985). The present result is about 17% higher than that of Tan *et al* (1974) and about 18% lower than that of Phillips *et al* (1985). Phillips *et al* (1985) reported that their measurements showed no dependence of the shape of

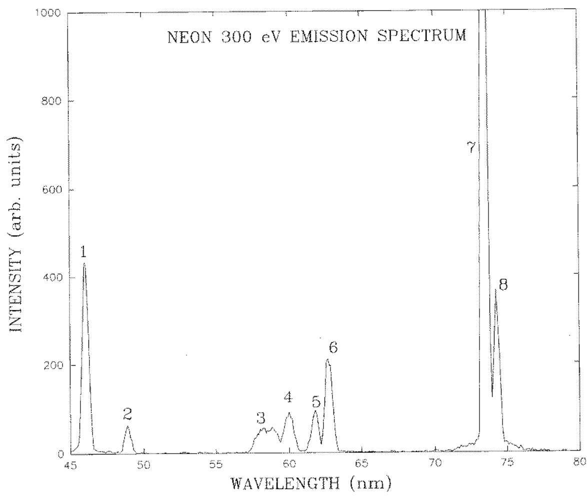

Figure 3. Calibrated, polarization-free electron-impact induced emission spectrum of Ne at 300 eV. The spectrum was obtained in the crossed-beam mode at 5×10^{-7} Torr background gas pressure. Emission cross sections for the identified features (numbered) are listed in table 1.

Table 1. Absolute emission cross sections of Ne at 300 eV.

Feature	Species	Integrated λ (nm)	Observed peak λ (nm)	Emission cross section ($\times 10^{-19}$ cm^2)
1	Ne II	45.1–47.1	46.1	15.3
2	Ne III	48.5–49.5	49.0	1.85
3	Ne I	57.3–59.5	58.9	5.67
4	Ne I	59.6–60.9	60.1	3.99
5	Ne I	61.2–62.3	61.9	3.29
6	Ne I	62.4–63.5	62.8	8.01
7	Ne I	71.4–74.1	73.6	53.2
8	Ne I	74.2–76.2	74.4	12.1

the excitation functions on pressure. They used a higher gas pressure in their measurements than that used by Hertz (1969). Hertz (1969) obtained his cross section value for the Ne I (73.6 nm) resonance transition for two different pressures ($P_1 = 2.7 \times 10^{-3}$ Torr and $P_2 = 0.3\text{–}0.8 \times 10^{-4}$ Torr). He reported that his cross section measurement showed a strong dependence on gas pressure due to the radiation trapping, and is about 1.7 to 2.4 times higher than the present result, depending on pressure.

The Ne I (74.4 nm) resonance transition represents the third strongest feature in the Ne EUV spectrum at 300 eV electron-impact energy. The present determination for the Ne I (74.4 nm) absolute emission cross section and that of Phillips *et al* (1985) agree fairly well. Their result is about 25% higher than ours. The present result is in excellent agreement with that of Hertz (1969) (disagreement is less than 1%). It is not clear to us why there is a very large discrepancy between our result and that of Hertz (1969) for the Ne I (73.6 nm) absolute emission cross section since the agreement between the two cross section measurements for the Ne I (74.4 nm) is found to be excellent.

The root-sum-square uncertainty in the absolute cross sections in this work is estimated as follows: (1) uncertainty of 35% in the relative calibration, (2) uncertainty of 22% in the

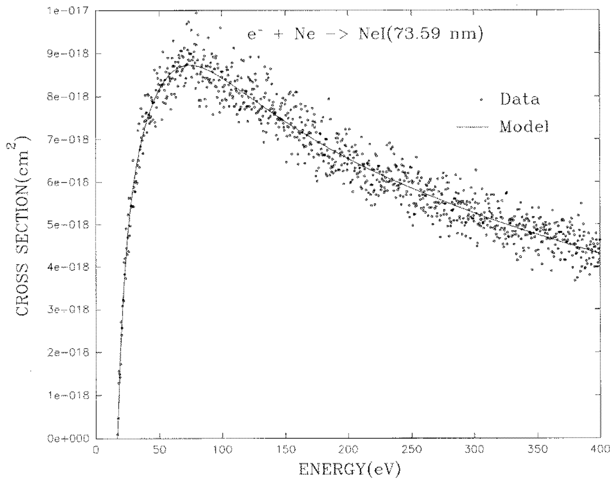

Figure 4. Relative emission cross section (optical excitation function) of the Ne I resonance line at 73.6 nm from 0–400 eV electron-impact energy. The data were corrected for polarization. The appearance potential is at 16.85 eV. The full curve represents a fitting function (Shemansky *et al* 1985a, b) to the data.

Table 2. Absolute emission cross sections of neon resonance transitions in the EUV (10^{-18} cm^2).

Energy (eV)	Ne I (73.69 nm)	Ne I (74.37 nm)	Ne II (46.07 + 46.24 nm)
20	2.55	1.32	—
30	6.05	2.31	—
40	7.44	2.30	—
50	8.18	2.29	—
60	8.56	2.28	0.20
70	8.71	2.26	0.37
80	8.70	2.22	0.55
90	8.59	2.15	0.71
100	8.42	2.08	0.86
125	7.92	1.90	1.16
150	7.41	1.74	1.35
175	6.95	1.61	1.47
200	6.55	1.51	1.53
250	5.86	1.34	1.56
300	5.27	1.21	1.52
350	4.76	1.10	1.51
400	4.30	0.99	1.46

N_2 (95.8 nm) emission cross section (Ajello *et al* 1989) and (3) signal statistics uncertainty of 3%. Thus the overall error (square root of the sum of the squares of the contributing errors) in the present cross section measurements is estimated to be about 41%.

3.2. Excitation functions

3.2.1. Ne I (73.6 and 74.4 nm) resonance lines. We show in figures 4 and 5 the excitation functions of Ne I 73.6 and 74.4 nm resonance transitions over the electron-impact energy range 0–400 eV. The excitation functions were corrected for polarization by use of the following formula (van der Burgt *et al* 1989):

$$\sigma_{ij}(E_0) = \frac{C[1 - P(E_0)/3]}{1 - P(E_0)\cos^2\theta} I(\theta) \qquad (2)$$

where $\sigma_{ij}(E_0)$ is the photoemission cross section at an electron impact energy (E_0), $P(E_0)$ is the polarization, $I(\theta)$ is the intensity of the emitted radiation at some angle, θ (where $\theta = 90°$ in our experimental set up) and C is a constant related to the electron beam current, number density of the target gas and the path length of the electron beam through the target. The polarization of radiation, $P(E_0)$, for each electron-impact energy was tabulated by Hammond *et al* (1989) in the energy range from threshold to 500 eV. They measured VUV polarization which represents the integrated radiation emitted following electron-impact excitation of He and Ne. We used their values to correct our measurements for polarization.

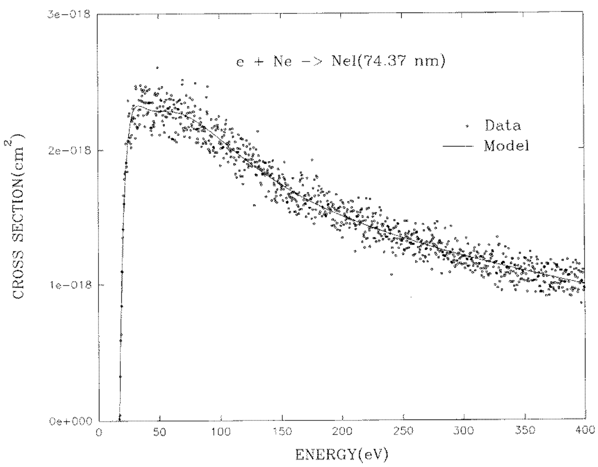

Figure 5. Relative emission cross section (optical excitation function) of the Ne I resonance line at 74.4 nm from 0–400 eV electron-impact energy. The data were corrected for polarization. The appearance potential is at 16.66 eV. The full curve represents a fitting function (Shemansky *et al* 1985a, b) to the data.

Figure 6 compares the present measurements of the Ne (73.6 nm) optical excitation cross sections with those of Phillips *et al* (1985), Hertz (1969), de Jongh (1971) and Tan *et al* (1974). All these measurements and ours include the cascade contributions from the upper levels. Integral cross sections for direct excitation (excluding cascade) reported by Register *et al* (1984) are also shown for comparison. Our results are in good agreement with those of Tan *et al* (1974) at all energies and with that of de Jongh (1971) at 200 eV. Both sets of results are lower in value than the present ones but lie well between the error limits of the present measurements as shown in figure 6. The cross sections of Phillips *et al* (1985) are higher than ours in the 40–300 eV energy range and the shape of their excitation function is different from ours. The discrepancy between the two data sets is worse in the peak region, and amounts to 70% at 40 eV. Measurements (with both low and high pressures) reported by Hertz (1969) are apparently too high. Direct excitation cross sections measured by Register *et al* (1984) agree reasonably well with the present measurements and lie within the quoted error limits at all overlapping energies. Disagreement reaches up to 30% in the peak energy region.

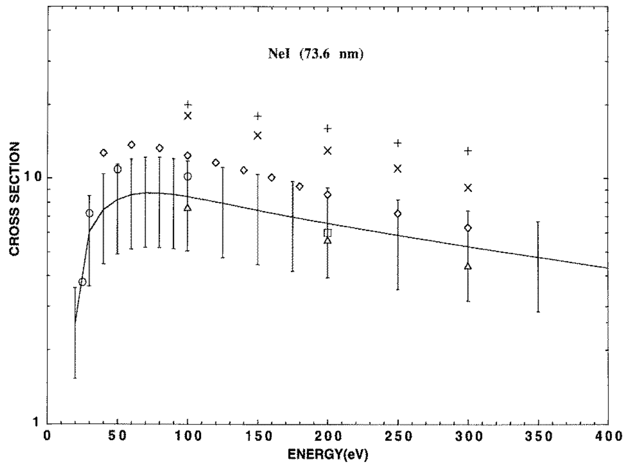

Figure 6. Comparison of published data for the cross section of the Ne I resonance line at 73.6 nm in the 0–400 eV energy range. The cross sections are given in the units of 10^{-18} cm^2. Measurements shown are: full curve, present data (error bars are also shown); $+$, Hertz (1969) high-pressure (2.7×10^{-3} Torr) data; $\times$, Hertz (1969) low-pressure ($0.3–0.8\times10^{-4}$ Torr); $\triangle$, Tan *et al* (1974); $\Diamond$, Phillips *et al* (1985); $\square$, de Jongh (1971); $\bigcirc$, Register *et al* (1984).

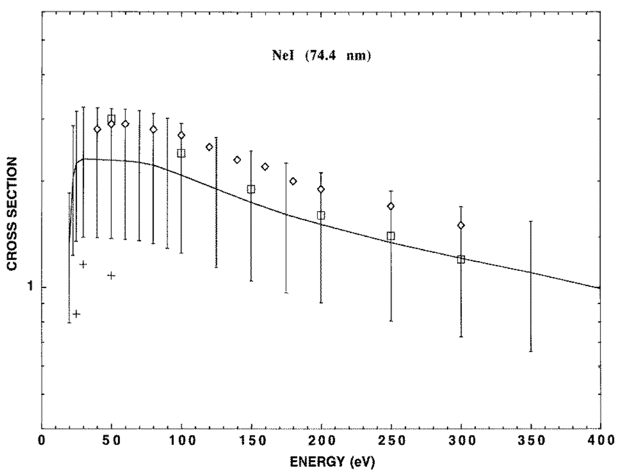

Figure 7. Comparison of published data for the cross section of the Ne I resonance line at 74.4 nm in the 0–400 eV energy range. The cross sections are given in the units of 10^{-18} cm^2. Measurements shown are: full curve, present data (error bars are also shown); $\square$, Hertz (1969); $\Diamond$, Phillips *et al* (1985); $+$, Register *et al* (1984).

The comparison of the present Ne (74.4 nm) optical excitation cross sections with those of Hertz (1969) and Phillips *et al* (1985) is given in figure 7. All emission cross sections include a substantial amount of cascade contributions from the upper levels. This situation is worse for the 74.4 nm emission line (about 50% of the total cascade has an optically allowed character) than for the 73.6 nm line (van Raan 1973). The Register *et al* (1984) integral cross sections for direct electron-impact excitation are also shown in figure 7. The cross sections of Phillips *et al* (1985) are much higher than ours (by up to a factor of 2) in the overlapping energy range. The disagreement between the two measurements is greater

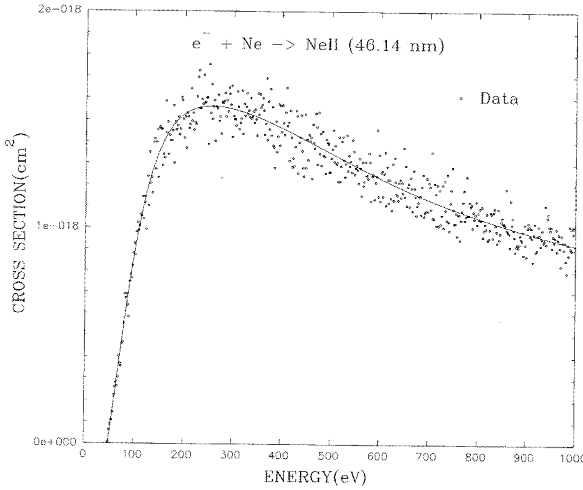

Figure 8. Relative emission cross section (optical excitation function) of the Ne II ion multiplet at 46.14 nm from 0–1 keV electron-impact energy. The appearance potential is at 48.43 eV. The full curve represents a fitting function (Shemansky *et al* 1985a, b) to the data.

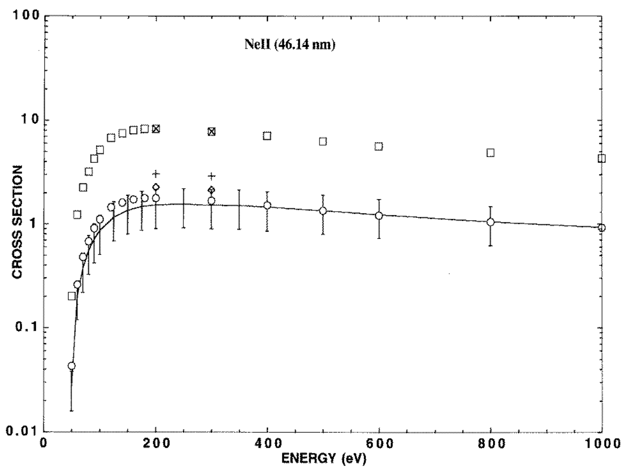

Figure 9. Comparison of published data for the cross section of the Ne II ion multiplet at 46.14 nm in the 1 keV energy range. The cross sections are given in units of 10^{-18} cm^2. Measurements shown are: full curve, present data (error bars are also shown); □, Luyken *et al* (1972); ○, Luyken *et al* (1972) normalized to present data at 500 eV; ◇, Dijkkamp and de Heer (1981); +, Eckhardt and Schartner (1983); ×, van Raan (1973).

for Ne I (73.6 nm) except that the shape of their excitation function is quite similar to ours. Measurements reported by Hertz (1969) agree well with ours in the higher energy region, but the agreement is much poorer in the peak region. The discrepancy between the direct excitation cross sections measured by Register *et al* (1984) and the other measurements is quite large. This large discrepancy may be accounted for by large cascade contributions to emission cross sections from the upper levels. Direct excitation cross sections of Register *et al* (1984) do not contain any cascade components and they were expected to be lower than the emission cross sections.

3.2.2. Ne II *(46.14) multiplet.* Figure 8 shows the unresolved multiplet of Ne II polarization-free excitation function over the energy range 0–1 keV. Figure 9 compares the present measurement for the Ne II optical excitation cross sections with those of Luyken *et al* (1972), van Raan (1973), Dijkkamp and de Heer (1981) and Eckhardt and Schartner (1983). As seen from the figure, the cross sections from van Raan (1973) and Luyken *et al* (1972), who used van Raan's measurement at 300 eV to put their cross sections on an absolute scale, are much higher than other reported measurementas. Dijkkamp and de Heer (1981) pointed out that extrapolation of van Raan's (1973) calibration down to 46 nm led to a significant error. The results from Zapesochnyi *et al* (1974), which are not shown in the figure, are almost 12 times higher than the present measurements. They calibrated their spectrometer against the data of van Raan (1973). We renormalized the Luyken *et al* (1972) results to our cross section at 500 eV. The renormalized cross sections of Luyken *et al* (1972) agree well with the present results especially in the high-energy region. Our results are approximately 1.5 to 2 times lower than those of Dijkkamp and de Heer (1981) and Eckhardt and Schartner (1983).

Acknowledgments

This work was carried out at the Jet Propulsion Laboratory, California Institute of Technology and was supported by the Air Force Office of Scientific Research (AFOSR), the Aeronomy Program of the National Science Foundation (grant no ATM-9320589), and NASA Planetary Atmospheres, Astronomy/Astrophysics and Space Physics Program Offices.

References

Ajello J M, James G K and Franklin B O 1989 *Phys. Rev.* A **40** 3524
Ajello J M *et al* 1988 *Appl. Opt.* **27** 890
Atreya S K 1986 *Atmospheres and Ionospheres of the Outer Planets* (New York: Springer)
Barger A J, Gallagher J S, Bjorkman K S, Johansen K A and Nordsieck K H 1993 *Astrophys. J.* **419** L85
Bartmess J E and Georgiadis R M 1983 *Vacuum* **33** 149
Bethe H 1930 *Ann. Phys., Lpz.* **5** 325
Chan W F, Cooper G. Guo X and Brion C E 1992 *Phys. Rev.* A **45** 1420
de Jongh J P 1971 *PhD Thesis* University of Utrecht, The Netherlands (unpublished)
de Jongh J P and van Eck J 1971 *Physica* **51** 104
Dijkkamp D and de Heer F J 1981 *J. Phys. B: At. Mol. Phys.* **14** 1327
Eckhardt M and Schartner K-H 1983 *Z. Phys.* A **312** 321
Hammond P, Karras W, McConkey A G and McConkey J W 1989 *Phys. Rev.* A **40** 1804
Heddle D W O and Gallagher J W 1989 *Rev. Mod. Phys.* **61** 221
Hertz H 1969 *Z. Naturf.* **24a** 1937
Huentis D L, Hill R M, Nakano H and Lorents D C 1978 *J. Chem. Phys.* **69** 5133
James G K, Kanik I and Ajello J M 1995 *Astrophys. J.* **455** 769
Kanik I, James G K and Ajello J M 1995 *Phys. Rev.* A **51** 2067
Kelly R L 1987 *J. Chem. Ref. Data* **16** 35
Kim Y K and Inokuti M 1968 *Phys. Rev.* **175** 176
Landini M, Fossi B C, Paresce F and Stern R 1985 *Astrophys. J.* **289** 709
Luyken B F J, deHeer F J and Baas R Ch 1972 *Physica* **61** 200
Machado L E, Leal E P and Csanak G 1984 *Phys. Rev.* A **29** 1811
Nighan W L 1981 *IEEE Trans. Electron Devices* **ED-28** 625
Papp W-F Z, Shevera V S and Zapesochnyi I P 1977 *JETP Lett.* **25** 29
Phillips M H, Anderson L W and Lin C C 1985 *Phys. Rev.* A **32** 2117
Register D F, Trajmar S. Steffensen G and Cartwright D C 1984 *Phys. Rev.* A **29** 1793
Shemansky D E, Ajello J M and Hall D T 1985a *Astrophys. J.* **296** 765

Shemansky D E, Ajello J M, Hall D T and Franklin B 1985b *Astrophys. J.* **296** 774
Shull J M 1993 *Phys. Scr.* T **47** 165
Tan K-H, Donaldson F G and McConkey J W 1974 *Can. J. Phys.* **52** 782
van der Burgt P J M, Westerveld W B and Risley J S 1989 *J. Chem. Ref. Data* **18** 1757
van Raan A F J 1973 *Physica* **65** 566
Zapesochnyi I P, Zhukov I G and Fel'tsan P V 1974 *Sov. Phys.–JETP* **38** 675